Radio Astronomy -
Polarized Radiation

- Polarization (monochromatic wave case)
  - consider at an arbitrary position (r=0)

$$E = E_0 e^{-i\omega t}$$
$$= (\hat{x}E_1 + \hat{y}E_2) e^{-i\omega t}$$

$$E_1 = A_1 e^{i\phi_1} \; and \; E_2 = A_2 e^{i\phi_2}$$
$$E_x = A_1 cos(\omega t - \phi_1) \; and \; E_y = A_2 cos(\omega t - \phi_2)$$

  - draw figure

$$E_{x'} = A_0 \; cos\beta \; cos\omega t \; and \; E_{y'} = -A_0 \; sin\beta \; sin\omega t$$
$$-\pi/2 \leq \beta \leq \pi/2$$

$$(\frac{E_{x'}}{A_0 \; cos\beta})^2 + (\frac{E_{y'}}{A_0 \; sin\beta})^2 = 1$$

Radio Astronomy -
Polarized Radiation

- Polarization and Stokes parameters (monochromatic wave case)

$$E_x = A_0(\cos\beta\ \cos\chi\ \cos\omega t + \sin\beta\ \sin\chi\ \sin\omega t)$$
$$E_y = A_0(\cos\beta\ \sin\chi\ \cos\omega t - \sin\beta\ \cos\chi\ \sin\omega t)$$

$$A_1\ \cos\phi_1 = A_0\ \cos\beta\ \cos\chi$$
$$A_1\ \sin\phi_1 = A_0\ \sin\beta\ \sin\chi$$
$$A_2\ \cos\phi_2 = A_0\ \cos\beta\ \sin\chi$$
$$A_2\ \sin\phi_2 = -A_0\ \sin\beta\ \cos\chi$$

$$I \equiv A_1^2 + A_2^2 = A_0^2$$
$$Q \equiv A_1^2 - A_2^2 = A_0^2\ \cos 2\beta\ \cos 2\chi$$
$$U \equiv 2A_1A_2\cos(\phi_1 - \phi_2) = A_0^2\ \cos 2\beta\ \sin 2\chi$$
$$V \equiv 2A_1A_2\sin(\phi_1 - \phi_2) = A_0^2\ \sin 2\beta$$

$$A_0 = \sqrt{I}$$
$$\sin\ 2\beta = \frac{V}{I}$$
$$\tan\ 2\chi = \frac{U}{Q}$$

$$I^2 = Q^2 + U^2 + V^2$$

Radio Astronomy -
Polarized Radiation

- Polarization
  - polarization measurement
    - Linear feeds or Circular feeds

Linear Polarization

$$
\begin{aligned}
S_0 &= I = E^2 = S \\
S_1 &= Q = I cos\ 2\chi \\
S_2 &= U = I sin\ 2\chi \\
S_3 &= V = 0
\end{aligned}
$$

Circular Polarization

right-handed (RCP)

$$S_0 = I = S$$
$$S_1 = Q = 0$$
$$S_2 = U = 0$$
$$S_3 = V = S$$

left-handed (LCP)

$$S_0 = I = S$$
$$S_1 = Q = 0$$
$$S_2 = U = 0$$
$$S_3 = V = -S$$

Radio Astronomy - Polarized Line Radiation

- Measuring magnetic fields - molecular line polarization
  - molecular line
    - Zeeman effect
      - Circular polarization
      - Zeeman, Lorentz (1902 Nobel prize)
        - line splitting
        - “strength” of B-field “along” the line of sight

Radio Astronomy - Polarized Line Radiation

Coutercy of Dr. C.C. Chiong

Zeeman effect

- Splitting of spectral lines into multiple components due to the coupling of an atom's or molecule's magnetic moment with an external magnetic field. σ+ and σ- has signals with different circular polarization. Different g factor for different molecules and transition.
- Suitable atoms or molecules are HI, OH, H_2O, CSS, CN, SO etc.

Most successful detection cases of Zeeman measurement are with HI, OH and H_2O.

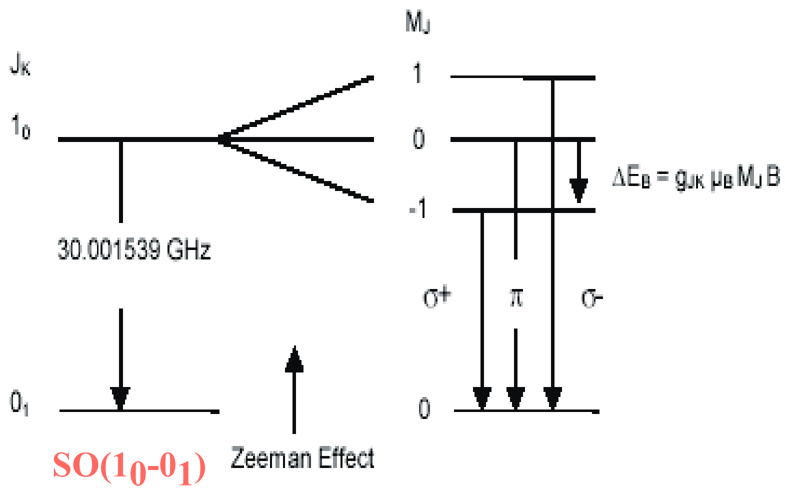

Radio Astronomy - Polarized Line Radiation

Coutercy of Dr. C.C. Chiong

Zeeman effect

- If the splitting is large (RCP, LCP well separated), the total field strength can be derived (only OH and H_2O maser).
- If the splitting is small, it provides only the „line-of-sight“ component B_{los}.

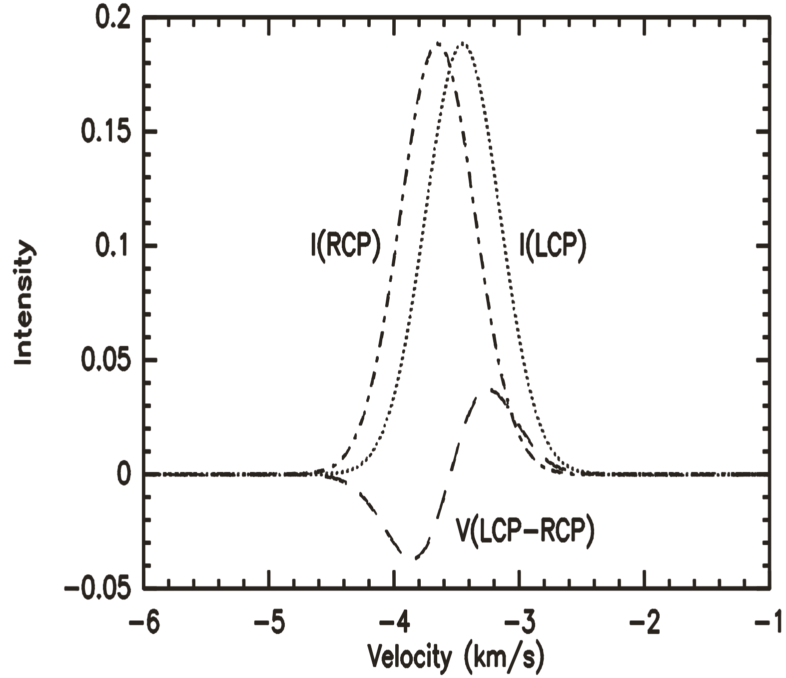

Radio Astronomy -
Polarized Line Radiation

Coutercy of Dr. C.C. Chiong

Zeeman effect

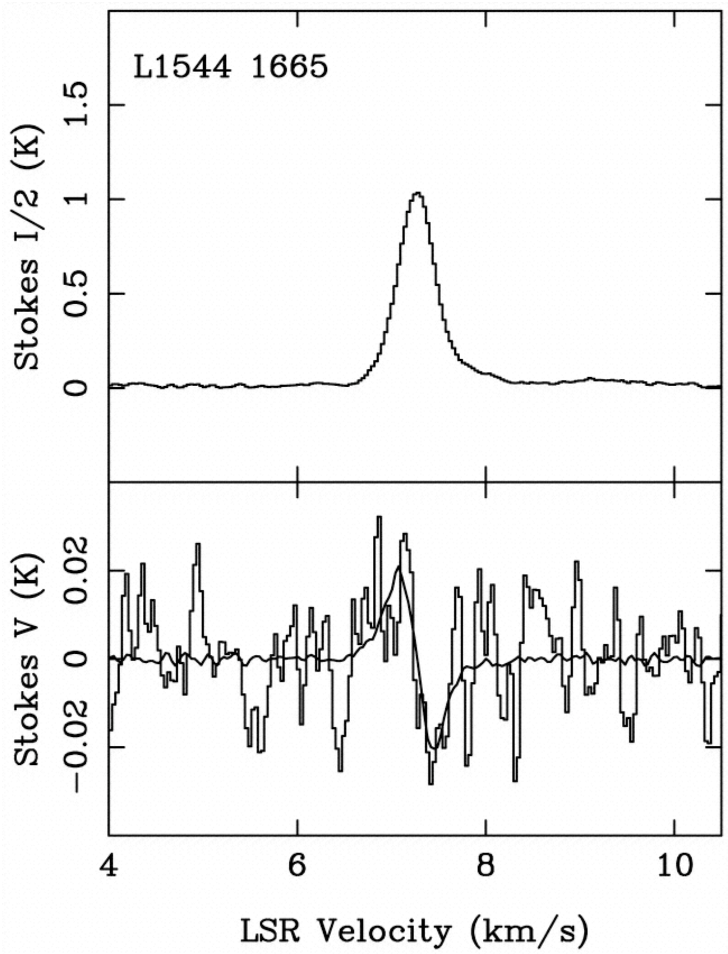

B(l.o.s.) ~ 10 micro Gauss

Crutcher and Troland 2000 ApJL

Radio Astronomy -
Polarized Line Radiation

Coutercy of Dr. C.C. Chiong

Current Status

• Bear in mind first that In most cases, only line-of-sight or plane-of-sky component is measured.

• Observational data supporting the existing star formation theories are still rare, because it is hard to measure the strength of interstellar magnetic fields.

Theories :

The B-ρ relation: $|B| \propto \rho\kappa$,

κ = 1/2 to 1/3 (Mouschovias, 1985)

Observations :

Crutcher (1999) reviewed 15 detections and 3 upper limits towards the dense region.

$B_{los} \propto \rho^{0.47\pm0.08}$

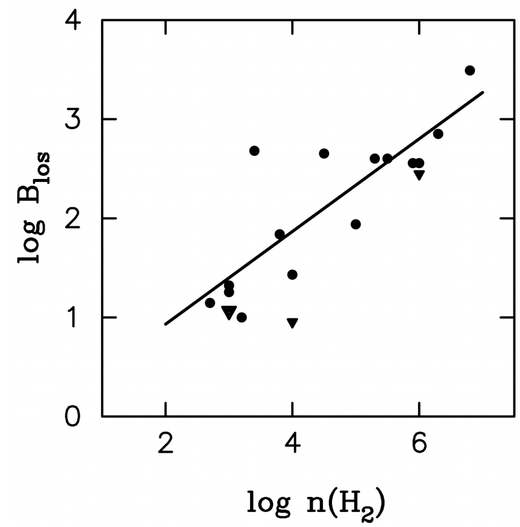

Radio Astronomy -
Dust Emission

- dust
  - continuum emission - modified blackbody radiation due to the wavelength dependence of dust grain emissivity.

$$\tau_{dust} \propto \nu^{\beta} \; with \; \beta \sim 1 - 2$$

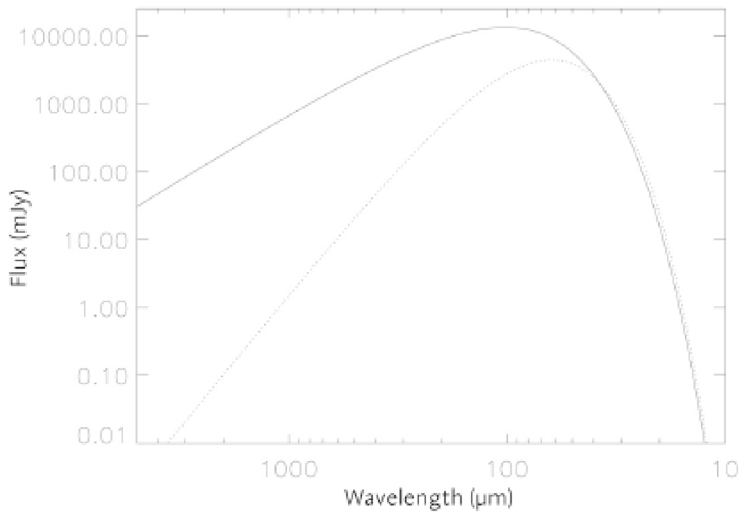

FIGURE 1 Comparison of flux emission between a blackbody (solid line) and a greybody (dotted line) for a fixed solid angle and temperature. Flux is given in units of milliJanskies, where 1 mJy = 10^{-29} W·m^{-2}·Hz^{-1}.

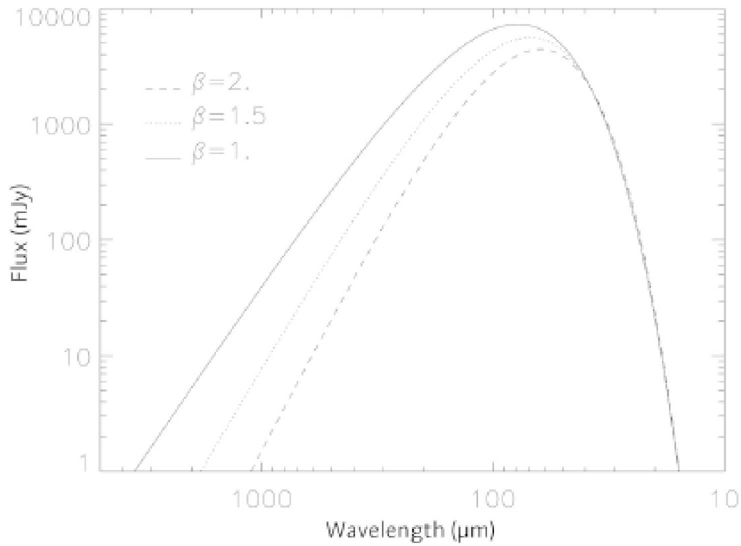

FIGURE 2 Greybody curve where β (unitless) is the varied parameter.

Radio Astronomy -
Dust Emission and Cores

- IRAM 30 m
- 37 (MAMBO-1)/117 (MAMBO 2) pixel bolometer array at 1.2 mm

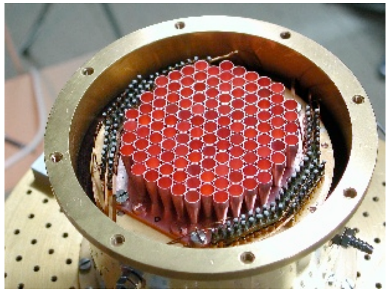

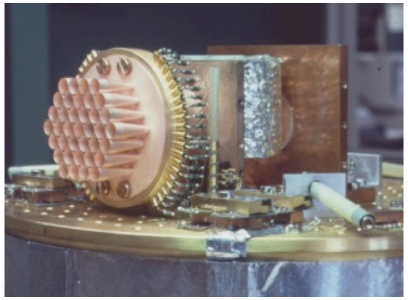

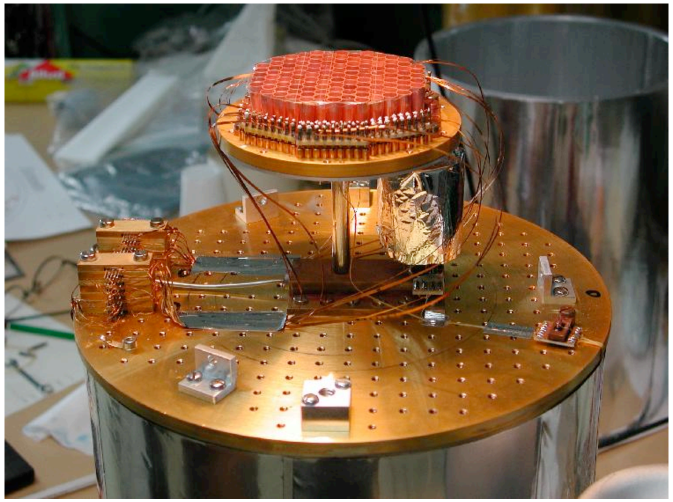

Radio Astronomy -
Dust Emission and Cores

- Dust in ρ Ophiuchus Star-Forming Region

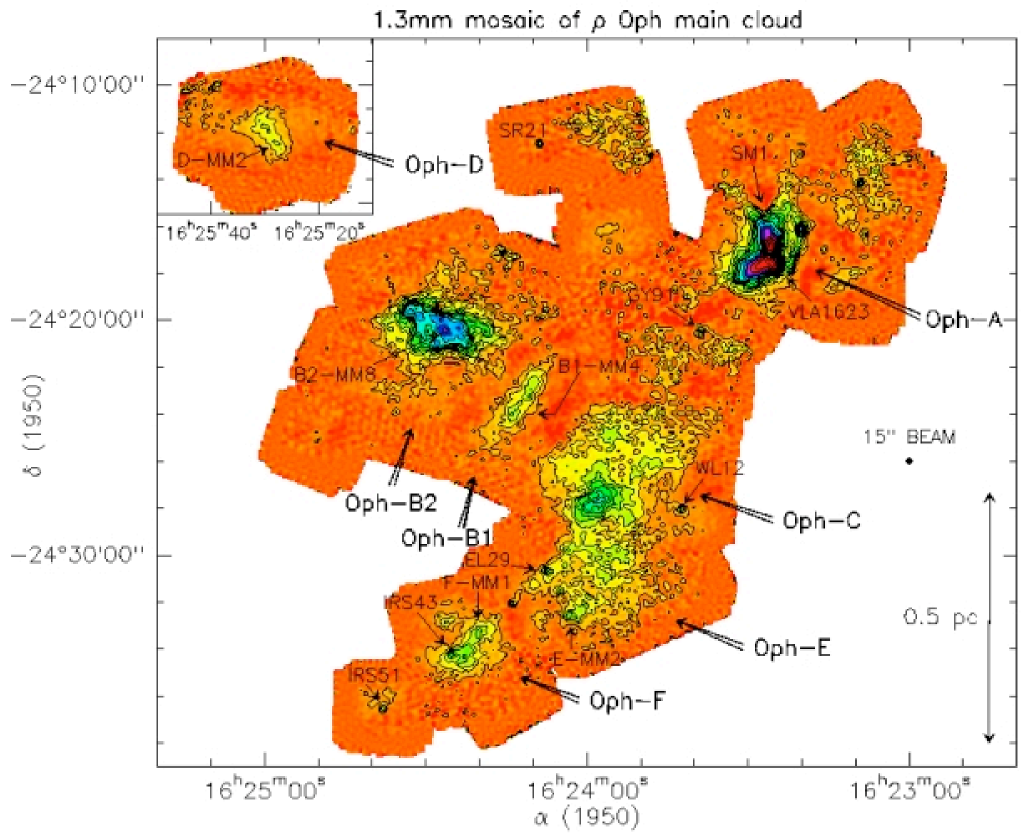

Motte et al. (1998)

Radio Astronomy - Polarized Dust Emission and Magnetic Field

- Measuring magnetic fields - dust continuum polarization
  - dust
    - continuum (emission/absorption; NOT scattered)
      - Linear polarization
      - due to alignment (see next page)
        - grain particles with magnetic moment (due to spinning) precess around the B-field
        - polarization provides the “direction” of B-field (perpendicular or parallel) “in” the plane of the sky
        - detail mechanism not secure
        - various competing processes including collision (temperature/density)

Radio Astronomy -
Polarized Dust Emission and Magnetic Field

- Dust continuum polarization mechanism
  - dust grain alignment (Lazarian, Goodman, Myers 1997, ApJ)

TABLE 1

MAJOR MECHANISMS OF GRAIN ALIGNMENT

Alignment Mechanism	Introduced	Description	Quantitative Theory	Special Conditions for Success
1. Gold	Gold 1951	Alignment of thermally rotating grains aligned by supersonic flows; *originally:* radiation pressure on grain; *further development:* Alfvénic waves (Lazarian 1994; Lazarian & Draine 1997b), ambipolar diffusion (Roberge et al. 1995)	Purcell 1969; Purcell & Spitzer 1971; Dolginov & Mytrophanov 1976; Lazarian 1994; Roberge et al. 1995; Roberge & Hanany 1990; Lazarian 1997a	Supersonic drift, rotation with thermal velocities
2. Mechanical alignment of suprathermally rotating grains	Lazarian 1995a	Alignment by suprathermally rotating grains by supersonic flows due to cross-section difference and due to gaseous bombardment during crossover events	Lazarian 1995a, 1995c; Lazarian & Efroimsky 1996; Lazarian, Efroimsky, & Ozik 1996	Supersonic drift, rotation with suprathermal velocities
3. Davis-Greenstein	Davis & Greenstein 1951	Alignment of thermally rotating grains through paramagnetic relaxation; *originally*: relaxation of paramagnetic grains; *further development*: relaxation of SPM grains (Jones & Spitzer 1967)	Jones & Spitzer 1967; Purcell & Spitzer 1971; Mathis 1986; Roberge et al. 1993; Lazarian 1995d; Lazarian & Roberge 1997a; Lazarian 1997b	Presence of SPM impurities
4. Purcell	Purcell 1975, 1979; Spitzer & McGlynn 1979	Alignment of suprathermally rotating grains through paramagnetic relaxation; *originally*: efficiency of alignment is limited for ordinary paramagnetic grains (Spitzer & McGlynn 1979); *further development:* incomplete Barnet relaxation enhances alignment (Lazarian & Draine 1997a)	Purcell 1979; Spitzer & McGlynn 1979; Lazarian 1995c, 1995e; Lazarian & Draine 1997a; Draine & Lazarian 1997a	Suprathermal rotation due to H_2 formation
5. Alignment by radiation torques	Draine & Weingartner 1996, 1997	Alignment due to the difference in scattering right and left polarized quanta	Draine & Weingartner 1996, 1997; Draine & Lazarian 1998	Radiation of short wavelength
6. Mechanical alignment of helical grains	Lazarian 1995b	Helical grains aligned by supersonic flows; atoms bounce off the grain surface of helical shape or off a grain with variation of the accommodation coefficient	Does not exist	Supersonic drift, special shape

Radio Astronomy -
Polarized Dust Emission and Magnetic Field

Radio Astronomy -
Polarized Dust Emission and Magnetic Field

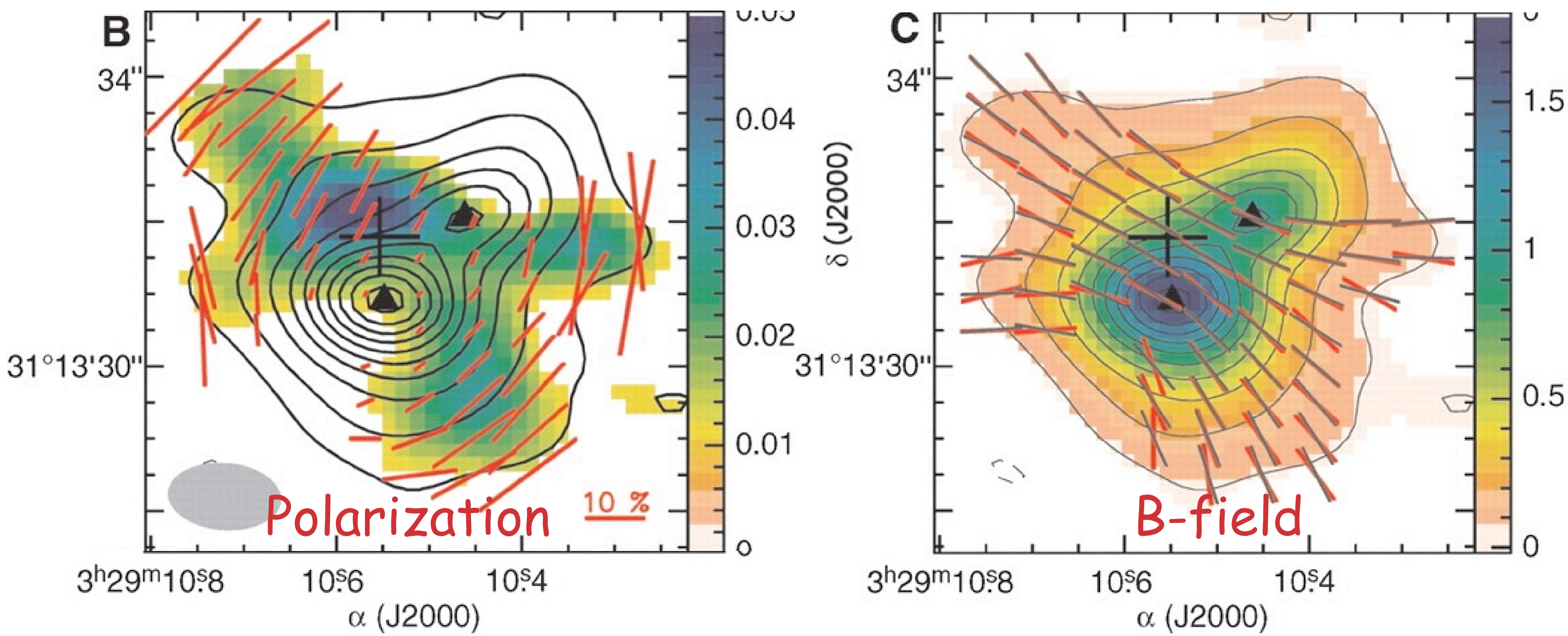

Girart, Rao, & Marrone 2006

Hour glass shape of the magnetic field structure in the circumbinary envelope

The large scale field is well aligned with the minor axis and the mass-to-flux ratio is slightly over critical

BEST OBSERVATIONAL CASE SO FAR!!!

Radio Astronomy -
Dust Emission and Star Formation at High z

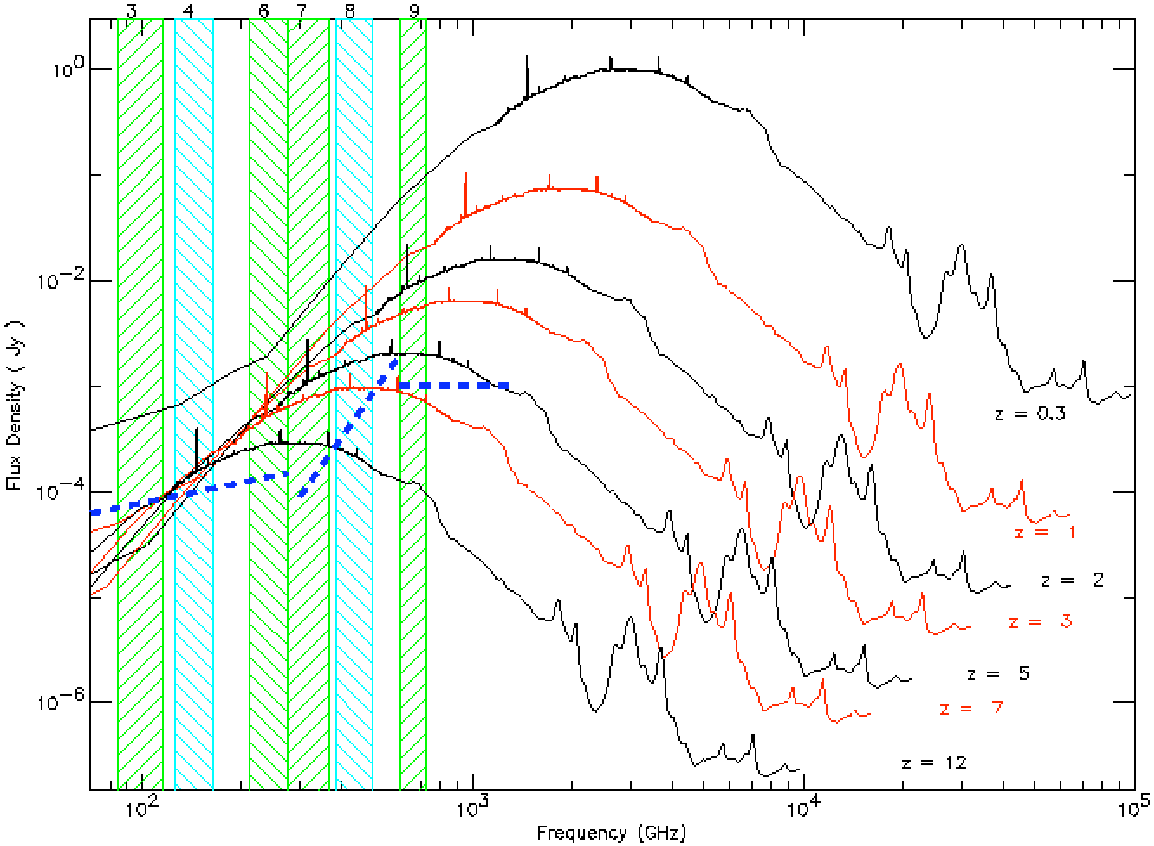

M82 from ISO, Beelen and Cox

Radio Astronomy -
Dust Emission and Star Formation at High z

- 37/9-pixel (SCUBA-1)/5100-pixel (SCUBA-2) bolometer array at 0.85/0.45 mm

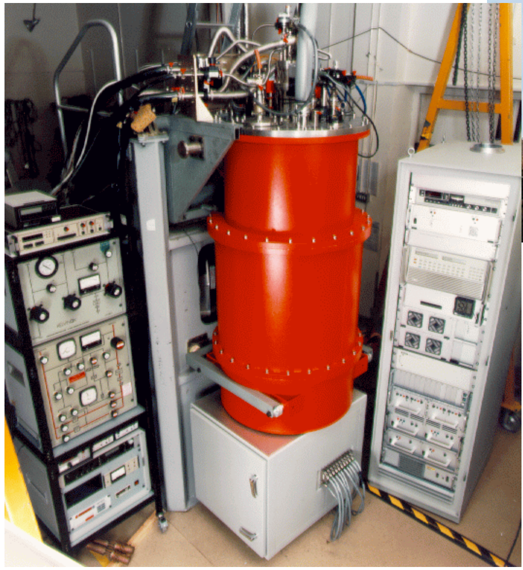

Radio Astronomy -
Dust Emission and Star Formation at High z

Dust emission from high-z galaxies in ongoing SHADES survey

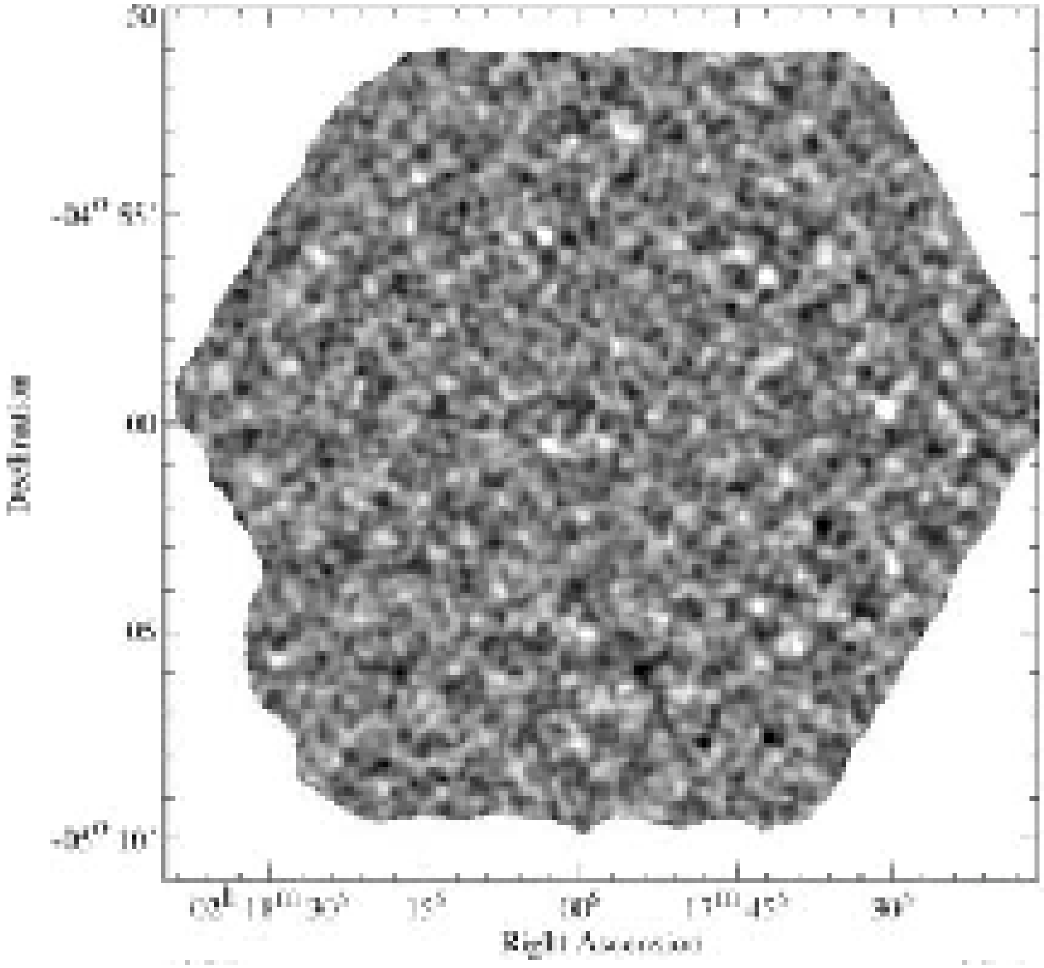

Coppin et al. (2006)

Radio Astronomy - Synchrotron Radiation and Pulsar Timing

- Binary Pulsar PSR 1913+16

- dish diameter of 305 m
- spherical dish, spherical aberration corrected inside Gregorian dome
- feeds illuminate 213x237 m of dish
- sky coverage -1° 20' ≤ δ ≤ 39° 02'
- nearly complete wavelength coverage from ~1 m (~300 MHz) to ~3 cm (~10 GHz)
- angular resolution from ~15' (at 1 m) to ~30" (at 3 cm)

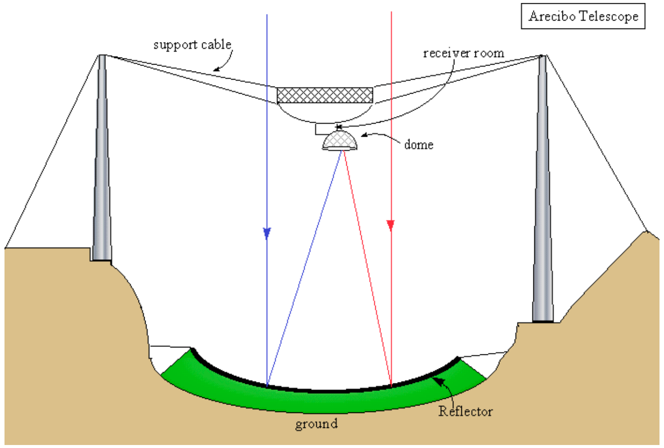

Radio Astronomy -
Synchrotron Radiation and Pulsar Timing

- Binary Pulsar PSR 1913+16

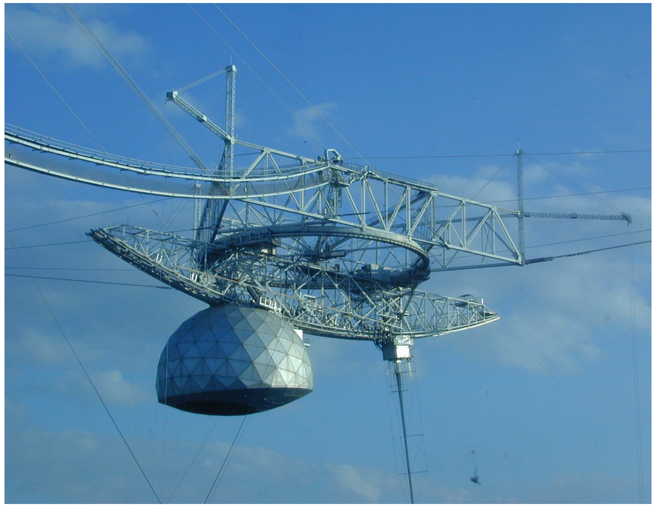

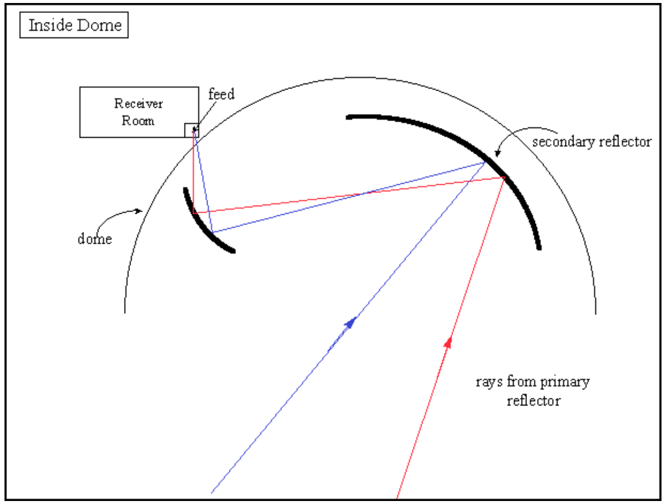

- dish diameter of 305 m
- spherical dish, spherical aberration corrected inside Gregorian dome
- feeds illuminate 213x237 m of dish
- sky coverage $-1° 20' \leq \delta \leq 39° 02'$
- nearly complete wavelength coverage from ~1 m (~300 MHz) to ~3 cm (~10 GHz)
- angular resolution from ~15' (at 1 m) to ~30" (at 3 cm)

Radio Astronomy -
Synchrotron Radiation and Pulsar Timing

- Binary Pulsar PSR 1913+16

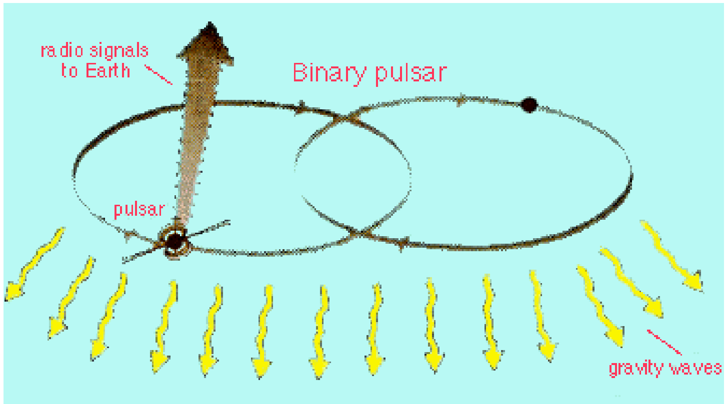

Comparison between observations of the binary pulsar PSR1913+16, and the prediction of general relativity based on loss of orbital energy via gravitational waves

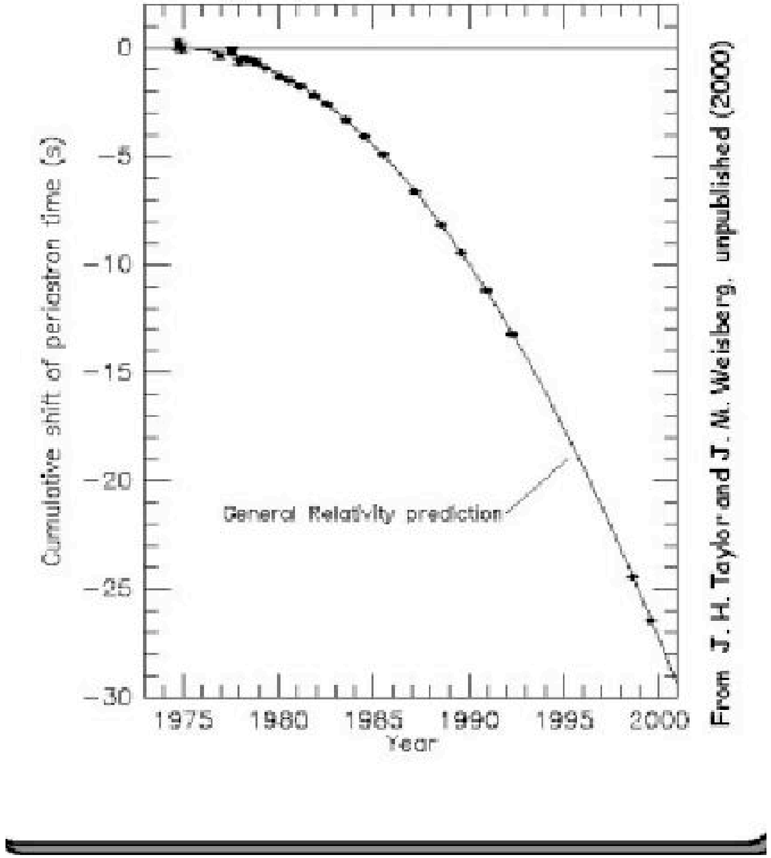

Radio Astronomy -
Radar Experiment

No H_2O ice in Lunar Craters

H_2O Ice in Craters on Mercury

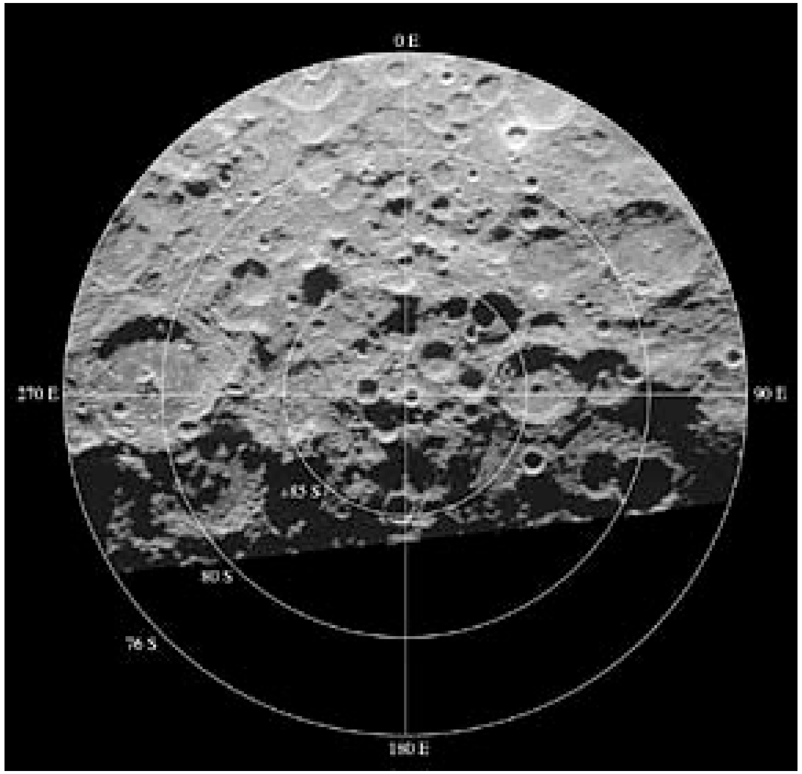

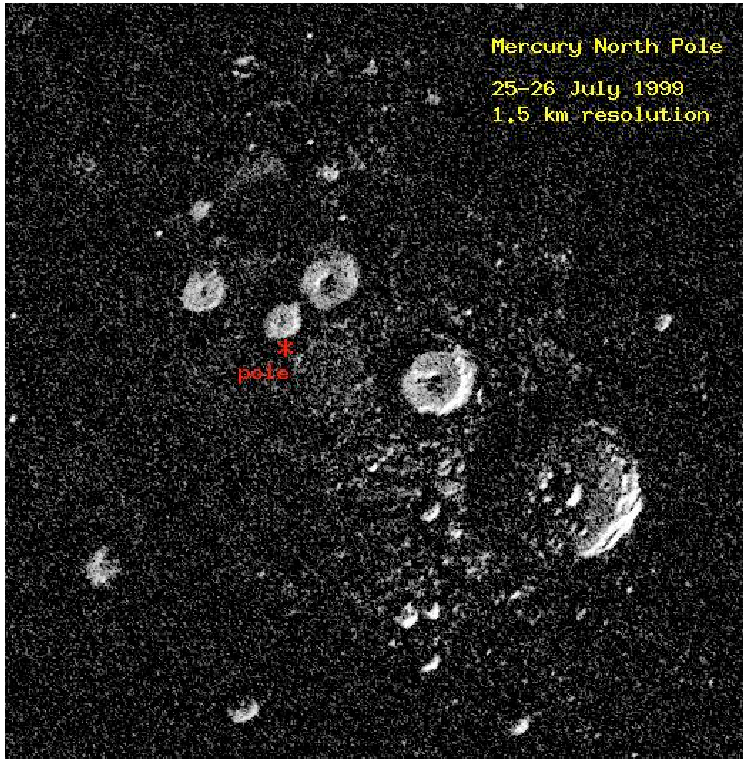

Radio Astronomy -
Synchrotron Radiation and AGN

- ten 25-m antennas
- wavelength bands 90, 50, 21, 13, 6, 4, 2, 1, 0.7 and 0.3 cm (0.3-90 GHz)
- dual polarizations
- maximum baselines of 8611 km
- angular resolutions as high as ~22 marcs at 90 cm to 72 μarcs at ~0.3 cm
- signals received at each antenna recorded on hard disk later correlated (VLBI) at Array Operations in Soccoro, New Mexico

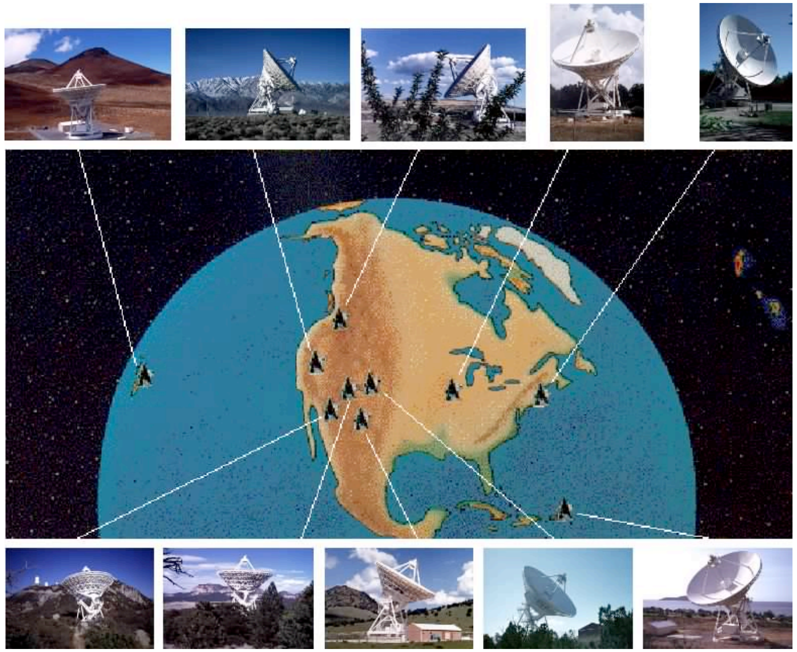

Radio Astronomy -
Synchrotron Radiation and AGN

- examples
  - radio galaxies and quasars (quasi-stellar radio sources)

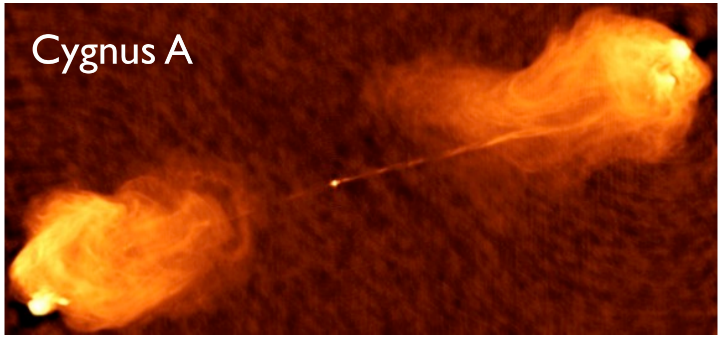

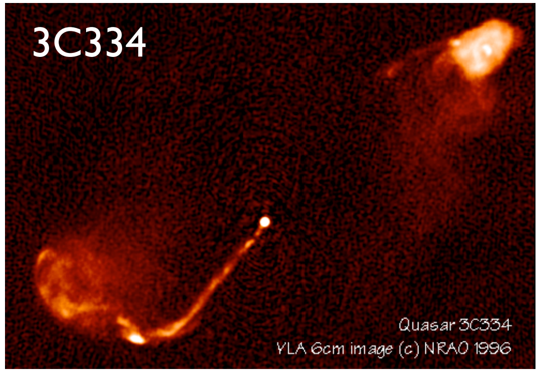

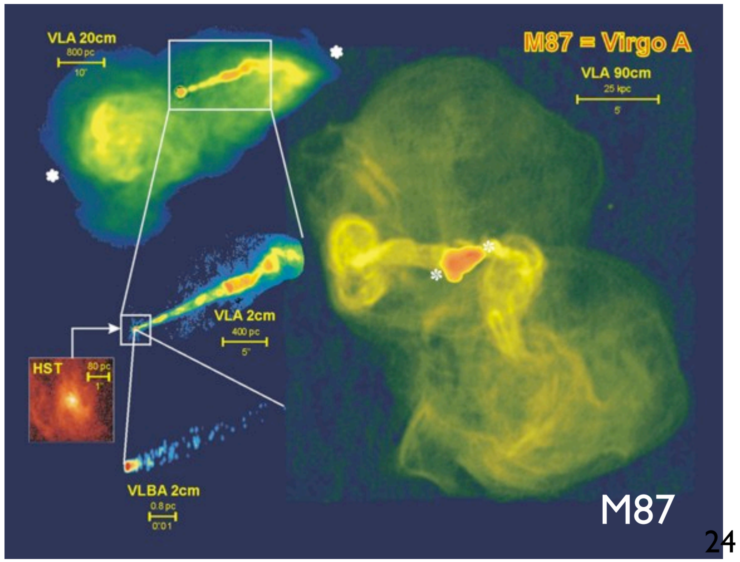

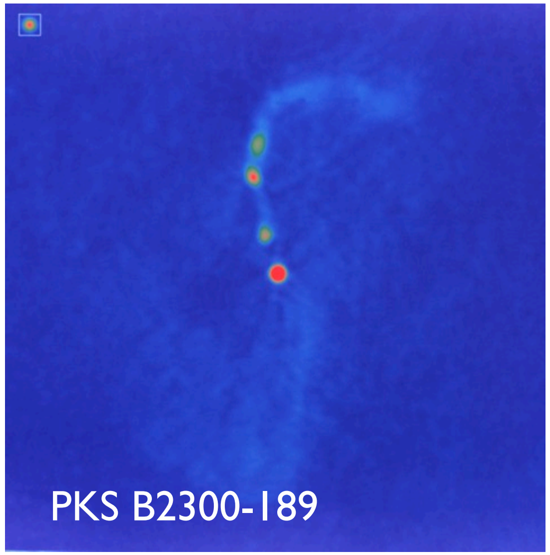

Radio Astronomy -
Synchrotron Radiation and AGN

Radio Jets from M87

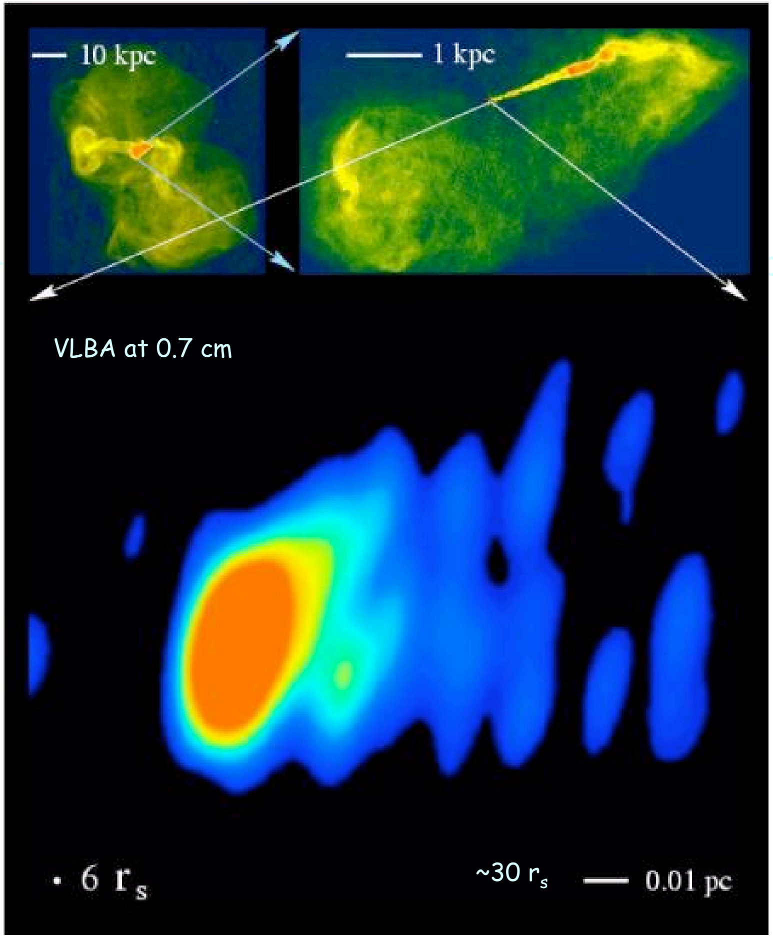

Junor et al. (1999)

Radio Astronomy -
Synchrotron Radiation and AGN

- radio jets and superluminal motion
  - 3C279 (25 light yrs in 7 yrs)

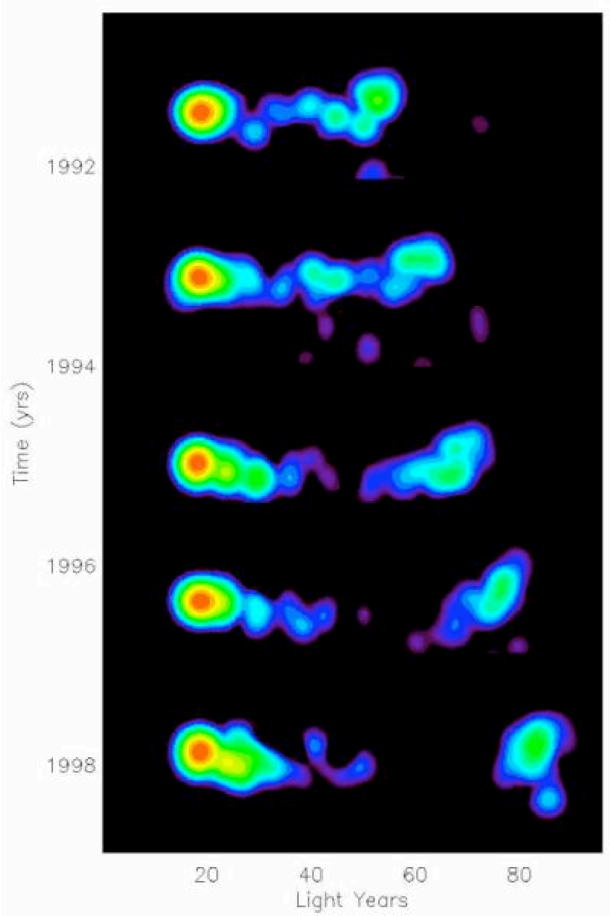

Radio Astronomy -
Synchrotron Radiation and AGN

- extragalactic radio sources
  - superluminal motion and relativistic beaming

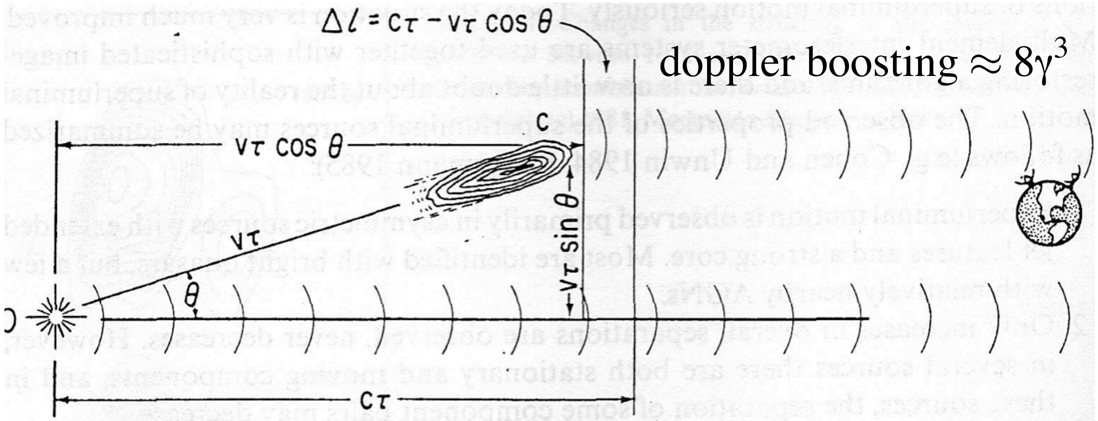

doppler boosting $\approx 8\gamma^3$

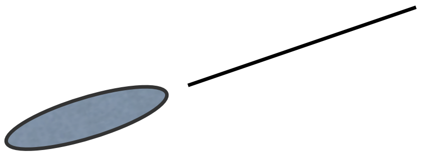

doppler boosting $\approx 1/8\gamma^3$

Fig. 13.8. Apparent superluminal motion results when the radiating source is moving so fast that it nearly catches up with its own radiation. Assume that a radiating plasma cloud is ejected from the origin, O, with a velocity v in a direction θ with respect to the line of sight. After a time t, the cloud has moved a distance vt. The motion, projected along the line of sight is $vt\cos\theta$, and projected perpendicular to the line of sight, $vt\sin\theta$. A distant observer sees the emission delayed by a time $t(c - v\cos\theta) = ct(1 - \beta\cos\theta)$ compared to the "signal" radiated when the cloud was at O. The apparent transverse velocity seen by the observer is then $(vt\sin\theta)/[ct(1 - \beta\cos\theta)] = \beta\sin\theta/(1 - \beta\cos\theta)$.

$$\upsilon_{app} = \frac{\upsilon\, sin\theta}{1 - \beta cos\theta}$$